Incorporation of Al or Hf in ALD TiO_2 for Ternary Dielectric Gate Insulation of InAlN/GaN and AlGaN/GaN MISH Structure

Running title: Incorporation of Al or Hf in ALD TiO_2 for Ternary Dielectric Gate Insulation of InAlN/GaN and AlGaN/GaN MISH Structure

Running Authors: Colon et al.

Albert Colon

University of Illinois at Chicago, Department of Electrical and Computer Engineering, Suite 1020 SEO, 10th Floor, 851 S Morgan St., Chicago, Illinois 60607

Liliana Stan, Ralu Divan

Argonne National Laboratory, Center for Nanoscale Materials, 9700 S-Cass Ave, Argonne, IL, 60439

Junxia Shi[a)]

University of Illinois at Chicago, Department of Electrical and Computer Engineering, Suite 1020 SEO, 10th Floor, 851 S Morgan St., Chicago, Illinois 60607

[a)] Electronic mail: lucyshi@uic.edu

This article investigates high dielectric constant gate insulators for GaN-based devices. Exploiting TiO_2 as a high-κ insulator typically compromises leakage current and temperature stability of the film. In this work we compare TiO_2 mixed with either Al_2O_3 or HfO_2 to form composite films Ti-Al-O and Ti-Hf-O, respectively, deposited by Atomic Layer Deposition (ALD) on both AlGaN/GaN and InAlN/GaN substrates. We investigated the compositional effects of the ternary compounds by varying the Al or Hf concentration, and we find that leakage current is reduced with increasing Al or Hf content in the film; with a maximum Al-content of 45 %, leakage current is suppressed by about 2 orders of magnitude while for a maximum Hf-content of 31 %, leakage current is suppressed by more than 2 orders of magnitude compared to the reference TiO_2

sample. Although the dielectric constant is reduced with increasing Al or Hf content, it is maintaining a high value down to 49, within the investigated compositional range. Crystallization temperature of the insulators were also studied and we found that the crystallization temperature depends on both composition and the content. For a Ti-Al-O film with Al concentration of 45 %, the crystallization temperature was increased upwards of 600° C, much larger compared to that of the reference TiO_2 film. The interface trap densities of the various insulators were also studied on both AlGaN/GaN and InAlN substrates. We found a minimal trap density of for the Ti-Hf-O compound with 35 % Hf. In conclusion, our study reveals that the desired high-κ properties of TiO_2 can be adequately maintained while improving other insulator performance factors. Moreover, Ti-Hf-O compounds displayed overall better performance than the Ti-Al-O composites.

I. INTRODUCTION

Gallium Nitride, a wide and direct bandgap semiconductor, has received much attention within the recent decades for transistors applications in high frequency power amplifiers[1] and high power switches[2]. However, the early transistors with Schottky-gates had problems such as current collapse and high gate leakage current. To relieve these problems, the Schottky-gate was replaced with a Metal-Insulator-Semiconductor-Heterojunction (MISH). Thus, there have been intense studies of insulator performance on GaN. A few desired properties of insulators include high dielectric constants[3], large

conduction and valence band offsets to the semiconductor[4], high crystallization temperature, low interface trap densities at the insulator/semiconductor interface and others. A high dielectric constant insulator is desired to maintain maximum channel control, increase AC transconductance[5] and minimize threshold voltage shift[3]. TiO_2 is attractive due to its high reported dielectric constant in the range of 60-120[6-8], however it suffers from high leakage current and low crystallization temperature of 370° C[9]. A method to improve these values while maintaining a high dielectric constant is by forming a ternary compound such as Ti-Al-O or Ti-Hf-O[10-12]. By creating these ternary compounds, adequate trade-offs with these factors can be obtained. For example, as depicted in Figure 1, although Al_2O_3 has a high crystallization temperature of 900° C[13], it has a low dielectric constant value of ~9[14]. TiO_2, being on the other half of these spectrums, exhibits the opposite behavior. Combining the two materials to create the ternary compound, Ti-Al-O, may allow for an adequate tradeoff in these factors under the 'compromise region' depicted in Figure 1. Another popular insulator, HfO_2, is also a potential material to create a ternary compound Ti-Hf-O. To date, there is limited published work investigating the performance of these ternary compounds on GaN semiconductors. To deposit these compounds, we used Atomic Layer Deposition (ALD), which is amongst the more popular insulator deposition methods due to its highly conformal process and its precise deposition control[15]. Moreover, ALD allows relatively easy control and engineering of multicomponent film composition, thus, a nanolaminate or composite film can easily be attained by changing the numbers of alternating cycles of each component. We investigate the compositional effects of either Al or Hf inclusion in TiO_2 by fabricating a MISH-capacitor structure using both AlGaN/GaN and InAlN/GaN

substrates. By varying the ALD cycle ratio of TiO_2 and either Al_2O_3 or HfO_2, the composition of each film was varied. It was found that there is an overall improvement in insulator performance with increasing Al or Hf content, compared to a reference TiO_2 film. Gate leakage current was reduced by more than 2 orders of magnitude for the Ti-Hf-O compound with 35% Hf. Dielectric constants of the ternary compounds were maintained at a high value with a minimum at 49. Through interface trap density analysis, our studies revealed that the Ti-Hf-O contained less interface traps than the Ti-Al-O compounds at . Post-deposition annealing of the films revealed that the crystallization temperature of the compounds was increased to up to more than 600° C for the Ti-Al-O film with 45 % Al.

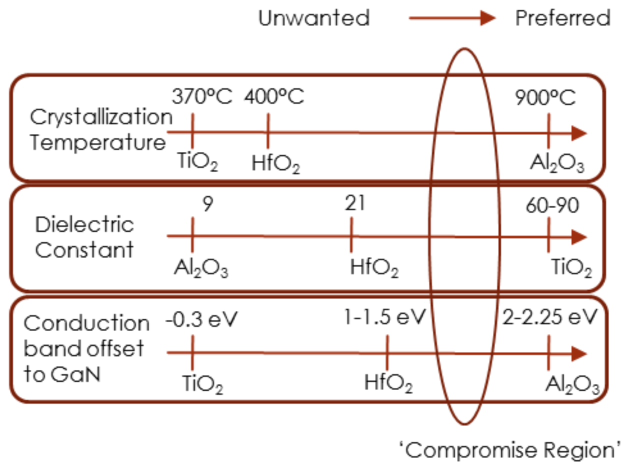

FIG. 1. (Color Online) Diagram representing some properties of commonly used dielectrics TiO_2, HfO_2 and Al_2O_3. Desired insulator properties include high crystallization temperature, large dielectric constant, and large conduction band offset to the semiconductor. Mixing TiO_2 with Al_2O_3 or HfO_2 creates ternary compounds Ti-Al-O or Ti-Hf-O, which may provide adequate tradeoffs in these respective properties under the 'Compromise Region'.

II. EXPERIMENTAL

To characterize the insulator qualities of Ti-Al-O and Ti-Hf-O on GaN, circular MISH capacitors were fabricated. A schematic cross-sectional image of the completed structure is shown in Figure 2. Device fabrication started with AlGaN/GaN on sapphire (consisting of 1.5 nm GaN cap, 21 nm $Al_{0.25}Ga_{0.75}N$ barrier, 1 nm AlN interbarrier layer, GaN channel layer, Sapphire substrate) and InAlN/GaN on SiC (consisting of 2.0 nm GaN cap, 5.0 nm $In_{0.17}Al_{0.83}N$ barrier, GaN channel layer, AlGaN back barrier, SiC substrate) epi-wafers provided by CorEnergy Semiconductor Technology Co. Ltd. and NXP Semiconductors, respectively, cleaned by ultrasonication in acetone followed by rinsing in methanol and isopropanol. Device isolation was achieved by Inductively-Coupled-Plasma Reactive Ion Etching (ICP RIE) (PlasmaLab 100 Oxford) using an $Ar/Cl_2/BCl_3$ chemistry plasma. Ohmic contacts were formed by lift-off of multi-layered stack of Si/Ti/Al/Ni/Au (1/15/90/45/55 nm) deposited by electron beam evaporation (PVD Varian). Thereafter, ohmic behavior was achieved by rapid thermal annealing at an optimized annealing condition at 825° C in N_2 for 30 s. The transfer length measurements (TLM) performed on-chip indicated an average contact resistance of 0.42 Ω·mm for InAlN and 0.48 Ω·mm for AlGaN.

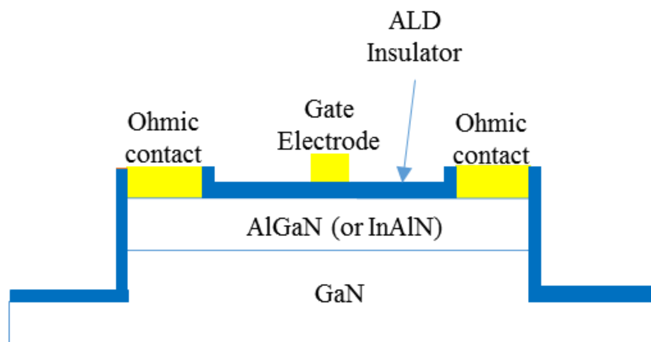

FIG. 2. (Color Online) Cross-sectional schematic of AlGaN(InAlN)/GaN MISH-Structure.

Following the ohmic contact formation, ternary dielectric deposition was achieved by thermal ALD (Arradiance Gemstar). The ALD films were deposited on InAlN/GaN, AlGaN/GaN, and Si witness samples. Prior to being loaded in the ALD chamber, the samples underwent a cleaning treatment consisting of buffered oxide etch 10:1 (NH_4F:HF = 90:10 %) dip followed by deionized water rinsing. The Ti-Al-O and Ti-Hf-O composite films were achieved by alternating TiO_2 and either Al_2O_3 or HfO_2 cycles. Each TiO_2, Al_2O_3, and HfO_2 cycles were carried out using tetrakis(dimethylamido)titanium (TDMATi)/H_2O, trimethylaluminum (TMA)/H_2O and tetrakis(dimethylamido)hafnium (TDMAHf)/H_2O, respectively. All films were deposited at 200° C at a deposition rate of 0.37 Å/cycle for TiO_2, 1.12 Å/cycle for Al_2O_3, and 0.85 Å/cycle for HfO_2. TiO_2 was deposited as a reference control sample. To vary the composition, 1 cycle of Al_2O_3 or HfO_2 was followed by a various number of consecutive TiO_2 cycles, i.e. 1-cycle of Al_2O_3 followed by n-cycles of TiO_2. The TiO_2:Al_2O_3 and TiO_2:HfO_2 cycle ratios studied were 10:1 and 5:1. Films of 2:1 cycles ratio were also deposited, however, because of the large Al or Hf concentrations in the films (>50 %), they are not of great interest for this particular study, in which a high Ti concentration and therefore high k value is desired. To achieve the final target thickness of ~15 nm, the super cycles were repeated. The thicknesses of the films were then measured by X-ray reflectivity (XRR) (Bruker D8 Discover) and the elemental composition was determined by X-ray photoelectron spectroscopy (XPS).

Following the insulator deposition, the gate contacts were patterned by e-beam lithography (Raith 150) using the bi-layer resist process, e-beam evaporation of Ti/Au (28/110 nm) and metal lift-off. Lastly, to make electrical contact to the covered ohmic

contact regions, the insulator films were etched from these regions using ICP RIE in an Ar/Cl_2-based plasma.

III. RESULTS AND DISCUSSION

Ti-Al-O and Ti-Hf-O films of compositions in the TiO_2-rich composition range were grown on the InAlN/GaN and AlGaN/GaN substrates. Their elemental compositions were evaluated from their XPS spectra and their thickness from their XRR spectra. The results are summarized in the Table I.

TABLE I. ALD films processing conditions, thickness and composition. 1:0 ratio (top row) is the reference TiO_2 film. The TiO_2 and Al_2O_3 or HfO_2 ratios were varied to produce different Al or Hf-content in the films.–

					Composition	
Ratio	TiO_2 cycle(s)	Al_2O_3/HfO_2 cycle	Ti-Al-O thickness (nm)	Ti-Hf-O thickness (nm)	Al-concentration($Ti_{1-x}Al_xO$)	Hf-concentration($Ti_{1-x}Hf_xO$)
1:0	1	0	13.6		0 % (TiO_2)	
10:1	10	1	17.0	13.4	36 % ($Ti_{64}Al_{36}O$)	18 % ($Ti_{82}Hf_{18}O$)
5:1	5	1	18.1	13.7	45 % ($Ti_{55}Al_{45}O$)	31 % ($Ti_{69}Hf_{31}O$)

The X-ray diffraction (XRD) measurements of as-deposited films revealed that the amorphous structure of as-deposited TiO_2, Ti-Al-O and Ti-Hf-O films persists in the whole investigated compositional range. To determine the temperature stability of the films, post-deposition annealing (PDA) was performed at various temperatures in O_2 ambient for 10 minutes and the XRD spectra measured thereafter and shown in Figures 3 and 4. The presence of the peaks at 25.17° corresponding to the anatase (101) TiO_2

structure in the XRD TiO_2 spectra shown in Figure 3, indicates that the films annealed at 350° C and above are crystalline. The other peaks present are the result of the diffraction from the sample holder and the silicon substrate as they are present during a bare Si/sample holder scan shown in Figure 3. After PDA at 450° C, the TiO_2:HfO_2 (10:1) starts to crystallize while the other composite films remain amorphous (Figure 4a). After PDA at 600° C, all composites except the TiO_2:Al_2O_3 (5:1) become crystalline (Figure 4b). In conclusion, the temperature stability of the composites is increased by adding Al or Hf in the TiO_2 and it is dependent on both the dopant type, whether it is Al or Hf, and the % composition.

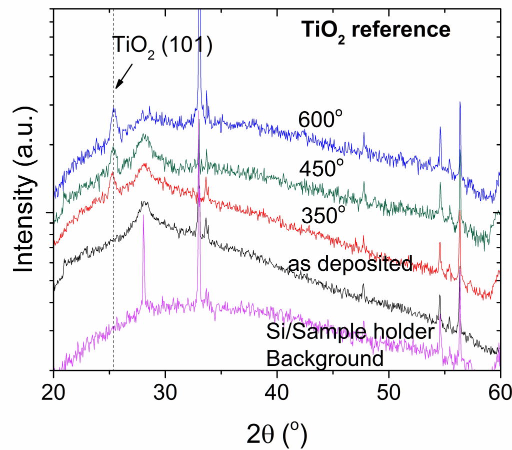

FIG. 3. (Color Online) XRD spectra of the TiO_2 reference sample. The bottom spectrum is a background scan from Silicon substrate and sample holder. Thereafter spectra correspond to as-deposited, annealed at 350° C, annealed at 450° C, and annealed at 600° C films.

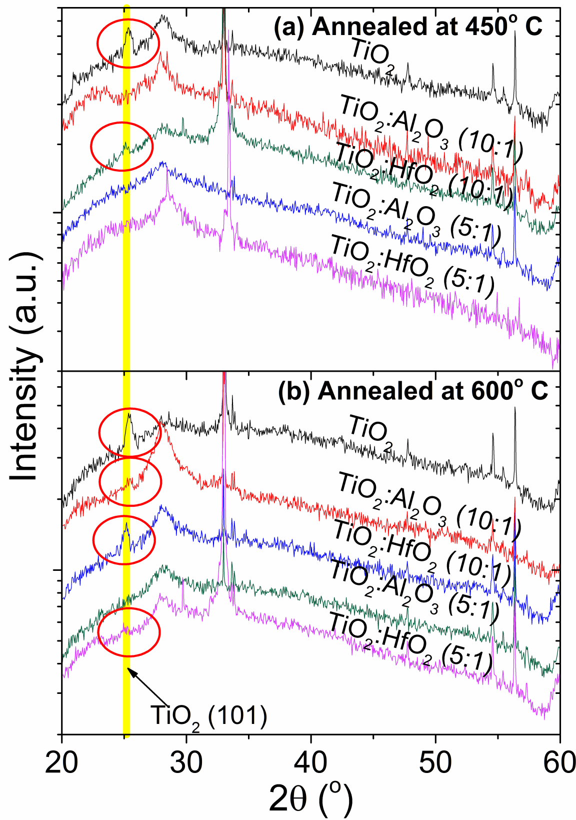

FIG. 4. (Color Online) XRD spectra of post-deposition annealed films. (a) After annealing at 450° C. (b) After annealing at 600° C.

The insulating properties of the ternary Ti-Al-O and Ti-Hf-O films grown on InAlN/GaN and AlGaN/GaN substrates were evaluated through current-voltage (I-V) measurements. Leakage current density was measured for both AlGaN/GaN and InAlN/GaN MISH capacitors and is plotted with gate voltage swept from -7 V to +1 V with a 0.1 V step size (Figure 5). Although the leaky TiO_2 reference sample shows a high leakage current density, these values are commonly reported in literature[10, 16, 17]. A decreasing overall trend in leakage current is observed with increasing Al or Hf-content in the films. Compared to the pure TiO_2 sample, leakage current was reduced about 2 orders of magnitude using a 5:1 cycles ratio TiO_2:Al_2O_3 composite film. However, the Ti-Hf-O compounds demonstrate lower leakage values than the Ti-Al-O compounds with

the lowest being about 3 orders of magnitude lower than TiO_2 measured on InAlN/GaN. The InAlN/GaN-based devices shows larger leakage values compared to AlGaN/GaN due to the thinner barrier layer and wider band-gap properties of the InAlN, which may create a lower conduction band offset to the insulator compared to AlGaN.

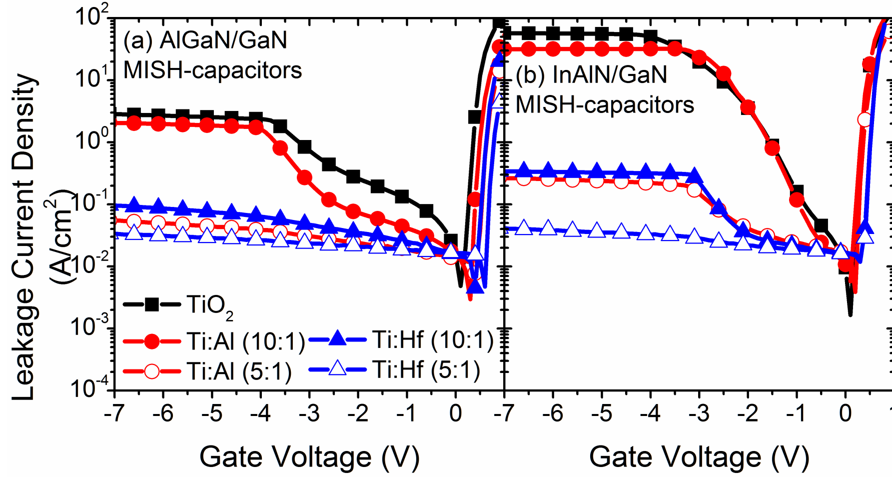

FIG. 5. (Color Online) Leakage current density of the ALD grown TiO_2 (black curves), Ti-Al-O (red curves) and Ti-Hf-O (blue curves) on (a) AlGaN/GaN and (b) InAlN/GaN as a function of gate voltage.

Figure 6(a) and 6(b) shows the capacitance-voltage (C-V) characteristics of the Ti-Al-O and Ti-Hf-O dielectrics measured on AlGaN/GaN (Figure 6a) and InAlN/GaN (Figure 6b) MISH capacitors, respectively. The voltage was swept from 0 V to -5 V using a 1 MHz AC signal with 10 mV amplitude and .05 V / 300 ms step size. A much sharper transition in the depletion region was observed for the 5:1 TiO_2:Al_2O_3 and TiO_2:HfO_2 cycle ratios sample compared to the TiO_2 reference sample on both substrates. A noticeable feature comparing the AlGaN/GaN and InAlN/GaN MISH capacitors is a much sharper C-V depletion region sweep for the former set of capacitors.

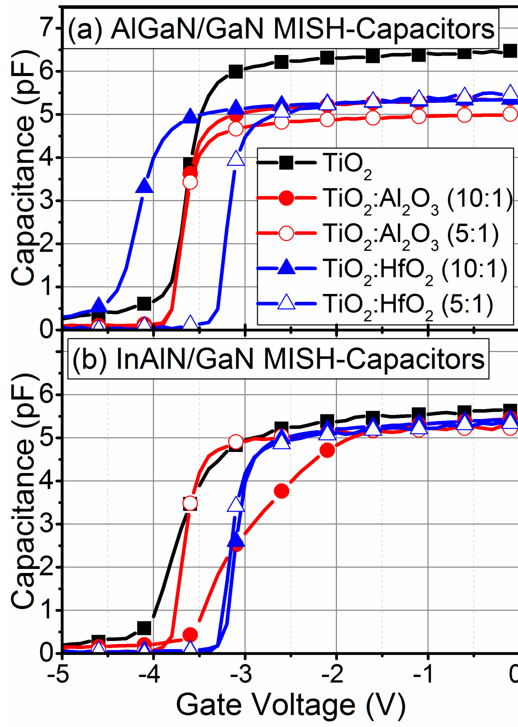

FIG. 6. (Color Online) C-V sweeps from 0 V to -5 V for the dielectrics measured on (a) AlGaN/GaN and (b) InAlN/GaN MISH capacitors. Measured using an AC signal with 1 MHz frequency, 10 mV amplitude and .05 V step size.

Dielectric constants were measured through the 0 V bias accumulation capacitance values. For the reference TiO_2 sample, a metal-insulator-metal capacitor was fabricated. From the capacitance measured at low voltage 10 kHz signal, the dielectric constant was directly measured to be 79 which matches well to other reported values[7, 8]. The relatively high dielectric constant of our ALD grown TiO_2 may be, to some degree, attributed to low film density[8]. That also influences the leakage current. Since the insulator forms a parallel plate capacitor in series with the barrier layer capacitance, the InAlN barrier layer capacitance can be calculated using the TiO_2 reference value. Thereafter, the remaining dielectric constant values were calculated from the InAlN MISH capacitors. The results are plotted in Figure 7. Mixing TiO_2 with Al_2O_3 or HfO_2

leads to a decrease in the dielectric constant, as expected. The dielectric constants of the Ti-Al-O and Ti-Hf-O composites studied here remain relatively high (around 50) compared to 9 or 21, as reported for Al_2O_3[14] and HfO_2[2], respectively. Counterintuitively, the k-values of the Al doped films are higher than the Hf doped counterparts. It has been shown that porous films with low density present high dielectric constant (particularly at a low frequency) and high leakage current density[8]. We believe that the Ti-Al-O composite films may be porous. This assumption is sustained by higher thickness of the Ti-Al-O films compared with the expected thickness according to the number of ALD cycles. Also, low-density Ti-Al-O films explain the higher leakage current densities measured on the Ti-Al-O MISH capacitors.

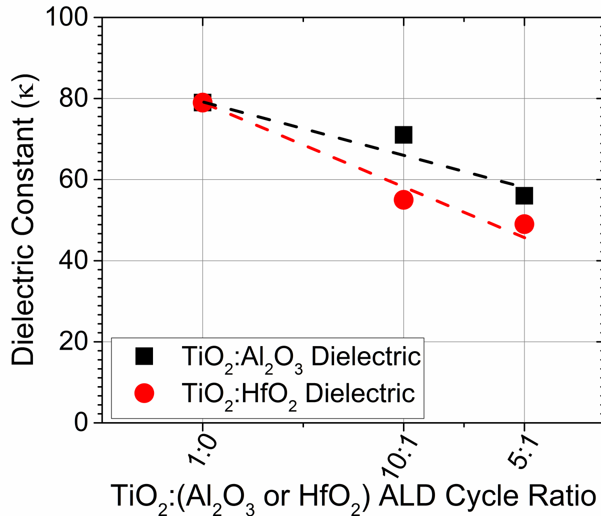

FIG. 7. (Color Online) Calculated dielectric constants of the Ti-Al-O and Ti-Hf-O films as a function of TiO_2:Al_2O_3/HfO_2 ALD cycle ratio. The dielectric constants are maintained at a relatively high value of 56 for TiO_2:Al_2O_3 (5:1) and 49 for TiO_2:HfO_2 (5:1).

A quantitative analysis of interface trap density (D_{it}) between the insulator and semiconductor is an important characteristic of the compatibility of an insulator on semiconductors. Interface trapped charges can be caused by several defects such as

structural defects, impurities and dangling bonds[18]. D_{it} values were extracted from the C-V frequency dispersion in the 2nd slope of the C-V sweep using a similar process as reported in literature[19-21]. As shown in Figure 8, a complete C-V curve features 2 slopes during a sweep. The 1st slope (at –bias) is associated with the accumulation of electrons at the InAlN(AlGaN)/GaN interface. The 2nd slope (at +bias) occurs due to the spill-over of electrons through the barrier layer onto the insulator/semiconductor interface. Based on the onset voltage shift in the 2nd slope (shown in Figure 8 inset) with measurement frequency change, D_{it} values may be extracted. By measuring the onset voltage shifts with respect to frequency, an average interface trap density may be extracted using:

Where C_{ox} is the insulator capacitance, q is the elemental electron charge, ΔV is the measured voltage hysteresis and ΔE is the corresponding trap energy difference. The corresponding trap energy difference can be calculated by:

Where k is Boltzmann's constant, T is the measurement temperature and f_i and f_{i+1} are the two different measurement frequencies. The corresponding average trap activation energy is calculated by:

where , interface traps capture cross section, , effective density of states in the barrier layer conduction band, and , thermal velocity of electrons, are assumed[22] to be $3.4 \cdot 10^{-15}$ cm^2, $2.2 \cdot 10^{18}$ cm^{-3} and $2.6 \cdot 10^7$ cm/s.

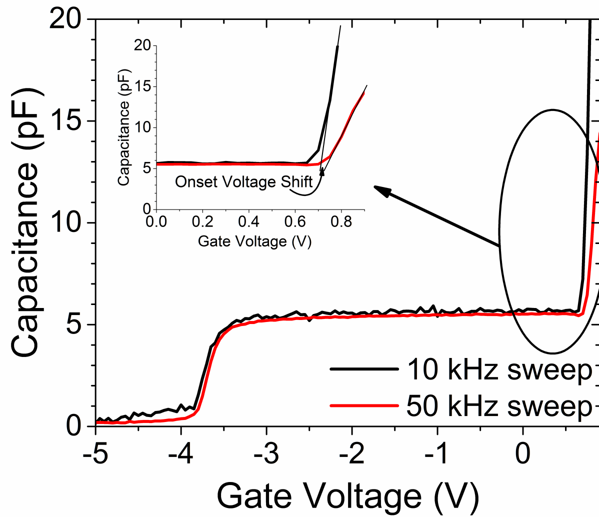

FIG. 8. (Color Online) Full C-V sweep of TiO_2:HfO_2 (5:1)/AlGaN/GaN MISH capacitor. The curve shows two slopes: the first at -4 V which is the accumulation of electrons at the 2DEG followed by the second slop at +0.7 V which is a result of electrons spillover from the 2DEG through the barrier layer and onto the insulator/semiconductor interface. Based on the onset-voltage shift when frequency is varied, interface trap density values may be extracted. The inset shows further detail on the 2nd slope's onset voltage shifts. Similar curves are measured for the rest of the MISH capacitors but are not shown.

The trap activation energy for the measured frequency range of 1kHz to 10kHz corresponds to 0.44 eV below the conduction band edge. The extracted D_{it} results are plotted in Figure 9. InAlN/GaN devices show larger trap densities compared to their AlGaN/GaN counterparts. However, the trap density appears to be decreasing with increasing Al or Hf-content in the film with the Ti-Hf-O compound exhibiting better performance than the Ti-Al-O compounds. Compared to values reported in literature for Al_2O_3 and HfO_2 on AlGaN/GaN[23, 24] larger than $4{\cdot}10^{13}$ $eV^{-1}cm^{-2}$, the ternary compounds appear to have lower trap densities. From the C-V analysis in Figure 6, it appeared that the TiO_2 sample showed larger stretch-out in the depletion region compared to the

compound films, suggesting a worse interface quality of the former, thus, the D_{it} analysis confirmed these results.

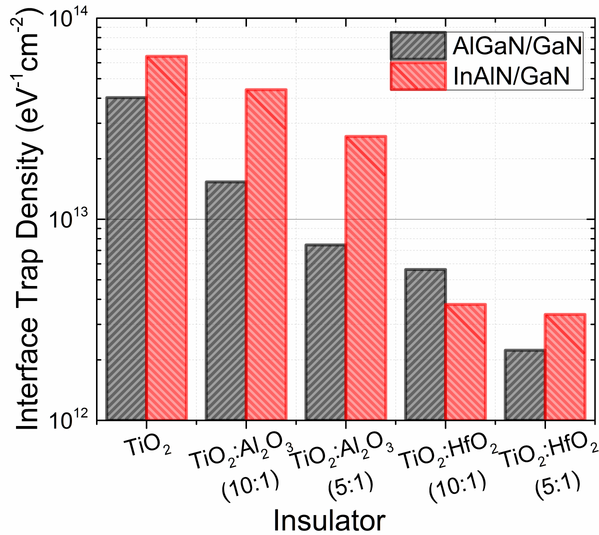

FIG. 9. (Color Online) Interface Trap Density measured from the various MISH capacitor structures through frequency-dependent C-V sweeps.

IV. CONCLUSIONS

We investigated the electrical properties of AlGaN/GaN and InAlN/GaN MISH capacitors employing ALD grown ternary Ti-Al-O and Ti-Hf-O compounds of various compositions as an insulator. It was revealed that by increasing the Al or Hf-content in the film, the leakage current was reduced as much as ~2-3 orders of magnitude for the Ti-Al-O, however, the Ti-Hf-O films showed the lowest leakage overall. Regarding the dielectric constant, the values were held high at 56 and 49 for the $Ti_{55}Al_{45}O$ and $Ti_{69}Hf_{31}O$ composites, respectively. It was shown that the crystallization temperatures of the composite films were increased substantially up to more than 600° C for the TiO_2:Al_2O_3 (5:1) film, compared to a crystallization temperature <350° C found for pure TiO_2. The

correlations between the interface trap-density of the films and the substrate material were also determined through C-V frequency dispersion measurements. The insulators deposited on InAlN/GaN showed larger interface trap densities compared to the AlGaN/GaN counterparts. While the ternary compounds showed improvement in this aspect with increasing TiO_2:Al_2O_3 or TiO_2:HfO_2 ALD cycle ratio, the Ti-Hf-O composites showed smaller trap densities compared to Ti-Al-O. In conclusion, we have demonstrated the performance of ternary insulator composites of various compositions on both AlGaN/GaN and InAlN/GaN substrates. Through our analysis, we have shown that the composites offer improved properties than TiO_2 while maintaining the attractive high-κ properties of this film. The Ti-Al-O composites offered a larger increase in thermal stability but the Ti-Hf-O films displayed lower leakage current and lower interface trapped charges.

ACKNOWLEDGMENTS

The authors would like to thank NXP Semiconductors for the financial support and CorEnergy Semiconductor Technology for the epi-structure supply. The authors would also like to thank Dr. Antonio Divenere and Dr. Seyoung An, staff at the Nanotechnology Core Facility (UIC), for their helpful discussions.

Use of the Center for Nanoscale Materials, an Office of Science user facility, was supported by the U. S. Department of Energy, Office of Science, Office of Basic Energy Sciences, under Contract No. DE-AC02-06CH11357.

[1]P. Saunier, M. L. Schuette, T.-M. Chou, H.-Q. Tserng, A. Ketterson, E. Beam, M. Pilla, and X. Gao, IEEE T. Electron. Dev. **60**, 3099-3104 (2013).
[2]J. Shi, L. F. Eastman, X. Xin, and M. Pophristic, Appl. Phys. Lett. **95**, (2009).
[3]T.-Y. Wu, C.-C. Hu, P.-W. Sze, T.-J. Huang, F. Adriyanto, C.-L. Wu, and Y.-H. Wang, Solid State Electron. **82**, 1-5 (2013).
[4]J. Robertson, and B. Falabretti, J. Appl. Phys. **100**, 014111 (2006).
[5]N. Ramanan, B. Lee, C. Kirkpatrick, R. Suri, and V. Misra, Semicond. Sci. Technol. **28**, 5 (2013).
[6]F. Takashi, and M. Hiroyuki, Jpn. J. Appl. Phys. **25**, 1288 (1986).

[7]F. Hisashi, N. Seigo, M. Miho, I. Yoshihiro, Y. Masaki, and N. Shigeru, Jpn. J. Appl. Phys. **38**, 6034 (1999).
[8]J. W. Lim, S. J. Yun, and J. H. Lee Electrochem. Solid St. **7**, F73-F76 (2004).
[9]Q. Xie, J. Musschoot, D. Deduytsche, R. L. Van Meirhaeghe, C. Detavernier, S. Van den Berghe, Y.-L. Jiang, G.-P. Ru, B.-Z. Li, and X.-P. Qu, J. Electrochem. Soc. **155**, H688-H692 (2008).
[10]A. Youngseo, M. Chandreswar, L. Changmin, C. Sungho, B. Young-Chul, K. Yu-Seon, L. Taeyoon, K. Jiyoung, C. Mann-Ho, and K. Hyoungsub, J. Phys. D Appl. Phys. **48**, 415302 (2015).
[11]J. W. Lim, S. J. Yun, and H. T. Kim, J. Electrochem. Soc. **154**, G239-G243 (2007).
[12]M. Liu, L. D. Zhang, G. He, X. J. Wang, and M. Fang, J. Appl. Phys. **108**, 024102 (2010).
[13]S. Jakschik, U. Schroeder, T. Hecht, M. Gutsche, H. Seidl, and J. W. Bartha, Thin Solid Films **425**, 216-220 (2003).
[14]S. Ganguly, J. Verma, G. Li, T. Zimmermann, H. Xing, and D. Jena, Appl. Phys. Lett. **99**, 193504 (2011).
[15]H. Tiznado, D. Dominguez, W. de la Cruz, R. Machorro, M. Curiel, and G. Soto, Rev. Mex. Fis. **58**, 459-465 (2012).
[16]W. Lehnert, G. Ruhl, and A. Gschwandtner, J. Vac. Sci. Technol. A **30**, (2012).
[17]L. C. Haspert, P. Banerjee, L. Henn-Lecordier, and G. W. Rubloff, J. Vac. Sci. Technol. B **29**, 041807 (2011).
[18]D. K. Schroder, *Semiconductor Material and Device Characterization*. (Wiley, Piscataway, NJ, 2006).
[19]M. Ťapajna, M. Jurkovič, L. Válik, Š. Haščík, D. Gregušová, F. Brunner, E.-M. Cho, T. Hashizume, and J. Kuzmík, J. Appl. Phys. **116**, 104501 (2014).
[20]X. Qin, A. Lucero, A. Azcatl, J. Kim, and R. M. Wallace, Appl. Phys. Lett. **105**, 011602 (2014).
[21]B. Qilong, H. Sen, W. Xinhua, W. Ke, Z. Yingkui, L. Yankui, Y. Chengyue, J. Haojie, L. Junfeng, H. Anqi, Y. Xuelin, S. Bo, L. Xinyu, and Z. Chao, Semicond. Sci. Technol. **31**, 065014 (2016).
[22]K. Zhang, J. S. Xue, M. Cao, L. Y. Yang, Y. H. Chen, J. C. Zhang, X. H. Ma, and Y. Hao, J. Appl. Phys. **113**, (2013).
[23]X. Y. Qin, L. X. Cheng, S. McDonnell, A. Azcatl, H. Zhu, J. Y. Kim, and R. M. Wallace, J. Mater. Sci.-Mater. El. **26**, 4638-4643 (2015).
[24]W. Jiechen, L. Xiaoxing, Y. Shenglin, J. Park, and D. Streit, presented at the Int. Rel. Phy., 2014 (unpublished).

TABLE I. ALD films processing conditions, thickness and composition. 1:0 ratio (top row) is the reference TiO_2 film. The TiO_2 and Al_2O_3 or HfO_2 ratios were varied to produce different Al or Hf-content in the films.–

	Composition

Ratio	TiO_2 cycle(s)	Al_2O_3/HfO_2 cycle	Ti-Al-O thickness (nm)	Ti-Hf-O thickness (nm)	Al-concentration($Ti_{1-x}Al_xO$)	Hf-concentration($Ti_{1-x}Hf_xO$)
1:0	1	0	13.6		0 % (TiO_2)	
10:1	10	1	17.0	13.4	36 % ($Ti_{64}Al_{36}O$)	18 % ($Ti_{82}Hf_{18}O$)
5:1	5	1	18.1	13.7	45 % ($Ti_{55}Al_{45}O$)	31 % ($Ti_{69}Hf_{31}O$)

FIG. 1. (Color Online) Diagram representing some properties of commonly used dielectrics TiO_2, HfO_2 and Al_2O_3. Desired insulator properties include high crystallization temperature, large dielectric constant, and large conduction band offset to the semiconductor. Mixing TiO_2 with Al_2O_3 or HfO_2 creates ternary compounds Ti-Al-O or Ti-Hf-O, which may provide adequate tradeoffs in these respective properties under the 'Compromise Region'.

FIG. 2. (Color Online) Cross-sectional schematic of AlGaN(InAlN)/GaN MISH-Structure.

FIG. 3. (Color Online) XRD spectra of the TiO_2 reference sample. The bottom spectrum is a background scan from Silicon substrate and sample holder. Thereafter spectra correspond to as-deposited, annealed at 350° C, annealed at 450° C, and annealed at 600° C films.

FIG. 4. (Color Online) XRD spectra of post-deposition annealed films. (a) After annealing at 450° C. (b) After annealing at 600° C.

FIG. 5. (Color Online) Leakage current density of the ALD grown TiO_2 (black curves), Ti-Al-O (red curves) and Ti-Hf-O (blue curves) on (a) AlGaN/GaN and (b) InAlN/GaN as a function of gate voltage.

FIG. 6. (Color Online) C-V sweeps from 0 V to -5 V for the dielectrics measured on (a) AlGaN/GaN and (b) InAlN/GaN MISH capacitors. Measured using an AC signal with 1 MHz frequency, 10 mV amplitude and .05 V step size.

FIG. 7. (Color Online) Calculated dielectric constants of the Ti-Al-O and Ti-Hf-O films as a function of TiO_2:Al_2O_3/HfO_2 ALD cycle ratio. The dielectric constants are maintained at a relatively high value of 56 for TiO_2:Al_2O_3 (5:1) and 49 for TiO_2:HfO_2 (5:1).

FIG. 8. (Color Online) Full C-V sweep of TiO_2:HfO_2 (5:1)/AlGaN/GaN MISH capacitor. The curve shows two slopes: the first at -4 V which is the accumulation of electrons at the 2DEG followed by the second slop at +0.7 V which is a result of electrons spillover from the 2DEG through the barrier layer and onto the insulator/semiconductor interface. Based on the onset-voltage shift when frequency is varied, interface trap density values may be extracted. The inset shows further detail on the 2nd slope's onset voltage shifts. Similar curves are measured for the rest of the MISH capacitors but are not shown.

FIG. 9. (Color Online) Interface Trap Density measured from the various MISH capacitor structures through frequency-dependent C-V sweeps.